



Original Paper

Assessment of Rockburst Risk in Deep Mining: An Improved Comprehensive Index Method

Qiming Zhang,^{1,2} Enyuan Wang,^{1,2,5} Xiaojun Feng,^{1,2,4,5} Chao Wang,^{1,3} Liming Qiu,^{1,2} and Hao Wang^{1,2}

Received 1 October 2020; accepted 15 December 2020
Published online: 5 January 2021

With the increasing depth of underground engineering, the risk of coal–rock dynamic disasters such as rockburst is becoming more and more serious and complex, which seriously threatens the safety of coal resource, mine production and the surface ecological environment. However, the existing risk indices and methods used for evaluating rockburst risk cannot be fully applied to deep coal seam group (DCG) mining. For the safe exploitation of coal resources, in this paper, based on statistical analyses of 300 cases of rockburst, six new indices are proposed for evaluating rockburst risk in the DCG, namely dip angle, moisture content, stability of coal seam, advancing speed of working face, disturbance factors and support patterns. In addition, the influence of multiple factors coupling and superposition on rockburst risk was considered. Thus, the Comprehensive Index Method of rockburst risk of Deep Coal seam Group (DCG–CIM) based on analytic hierarchy process was established. Finally, rockburst risk in the evaluation area was quantitatively assessed into four grades, including “No rockburst risk”, “Weak rockburst risk”, “Medium rockburst risk” and “Strong rockburst risk”. Taking the 2233 working face of Hengda Coalmine as an example, the evaluation results show that the ranges of 0–184 m, 224–284 m, 324–384 m, 424–484 m, 524–584 m and 594–624 m from terminal line of haulage roadway on 2233 working face were the medium rockburst risk zones, which are in accordance with the on-site impact damage results and are more accurate than the traditional method. The DCG–CIM can consider more inducing factors and obtain more accurate and reliable evaluation results and is more suitable for deep coal seam group mining.

KEY WORDS: Coal resource, Rockburst, Deep mining, Comprehensive index method, Numerical simulation.

INTRODUCTION

Rockburst, which usually causes injury to workers and damage to equipment, and even surface subsidence, is a common instability mode in coalmines (He et al. 2015; Bräuner 2017; Cheng et al. 2020; Hussain and Luo 2020; Zhang et al. 2020). In recent years, with the increase in mining depth, the characteristics became obvious, involved in deeply buried depth, high stress concentration, strong disturbance and complex stope structure, and

¹Key Laboratory of Gas and Fire Control for Coal Mines, China University of Mining and Technology, Ministry of Education, Xuzhou 221116, China.

²School of Safety Engineering, China University of Mining and Technology, Xuzhou 221116, China.

³School of Land and Resources Engineering, Kunming University of Science and Technology, Yunnan 650031, China.

⁴Henan Shenhua Grp Co Ltd, Yongcheng 476600, China.

⁵To whom correspondence should be addressed; e-mail: wey1top@cumt.edu.cn, xiaojun.feng@cumt.edu.cn

the intensity of rockburst increases continuously. On October 20, 2018, for instance, a rockburst accident occurred in the Longyun Coal Industry Co., Ltd., Shandong Province, China; it killed 21 people. Therefore, accurately evaluating dangerous areas in deep coal seam group (DCG) mining is a vital prerequisite for the development of reasonable and effective rockburst prevention measures, which is of great significance for guiding the safe production.

It is full of challenge to obtain the exact mechanism of rockburst in the DCG, because it is not only related to the inherent characteristics of coal–rock mass but also closely connected to high stress concentration and strong disturbance stress in coalmines (Dou and He 2004; Li et al. 2018; Kong et al. 2019; Qiu et al. 2020). Large-scale and high-intensity activities in the DCG result in frequent dynamic disturbances such as the roof weighting and mining earthquake. Moreover, the surrounding rock that has experienced the peak of high stress concentration will present a strong unloading effect after mining. In addition, combined with the increase in geo-stress and karst water pressure, the effective stress of deep coal–rock structure increases. The combined stress will accelerate the process of damage, deformation and instability of the primary cracks and joint in coal–rock. In addition, this phenomenon is more obvious in larger dip angle, lower moisture content and inhomogeneity coal seams, which can easily lead to dynamic disasters such as rockburst.

Up till now, there have been many studies on process analysis, evaluation and prediction of rockburst using experimental and theoretical analyses. He et al. (2010) analyzed the effect of geological and mining technical factors on the occurrence of rockburst and used the Comprehensive Index Method (CIM) to classify risk grades of rockburst and achieved good results in the field application. By analyzing uncertain information of rockburst risk in deep mining, Wang (2011) determined different index weights and constructed the unascertainable measurement model to evaluate rockburst risk. Pan and Xie (2012) proposed three new indicators, namely impact energy velocity index, critical softening region coefficient and critical stress coefficient, considering the time effect, and combined with four traditional indicators to evaluate the potential risk of rockburst. He et al. (2017) used the microseismic method to evaluate and predict rockburst by recording the released energy of mining earthquake and analyzing the occurred position of earthquake

activities. Song et al. (2017) used electromagnetic radiation (EMR) and acoustic emission (AE) to monitor the change trend of elastic energy in the impact process of coal–rock mass and proposed the energy discrimination method to achieve noncontact and continuous prediction of rockburst in deep mining. Based on the analysis of several rockburst accidents, Afraei et al. (2018) used quantitative theory to evaluate rockburst risk, which shows relatively high accuracy for the evaluation results. Cai et al. (2018) proposed five indicators, namely dynamic failure time, elastic energy index, impact energy index, uniaxial compressive strength and bending energy index, to evaluate the bursting liability of coal–rock mass through laboratory experiments. It can be seen from above that scholars have attained plenty of achievement in the risk evaluation of rockburst. However, the existing evaluation methods cannot cope well with complex stopes in the DCG owing to the fact that the present traditional evaluation system has ineluctable limitations; for examples, the evaluation indicators system is not comprehensive, the weight of evaluation index is unreasonable and the evaluation results of complex stope environment are not accurate enough.

Therefore, this paper analyzes rockburst accidents in recent years and six new evaluation indices, namely dip angle, moisture content, stability of coal seam, advancing speed of working face, precipitating factors and support patterns. Considering many factors in the mining process, the DCG–CIM is proposed to evaluate rockburst risk. The effectiveness of the DCG–CIM was verified by using the “8.6” rockburst accident, which occurred at the 2233 working face of the Hengda Coalmine.

EVALUATION METHOD

Survey and Statistical Analysis

In the evaluation process of rockburst risk, especially involved in the DCG, geological and mining factors are complex and diverse. For accurate and effective evaluation of rockburst risk, this paper analyzed several rockburst accidents including those in the Datong Xinzhouyao Coalmine, Hegang Junde Coalmine, Fushun Laohutai Coalmine, Fuxin Hengda Coalmine, Xuzhou Sanhejian Coalmine and some other coalmines (Xie et al. 1999; Li et al. 2007, 2016; Wang 2011; Feng and Zhang 2018; Liu and Wang 2018; Wang et al. 2019), summed up a lot of

Table 1. Statistics of factors that affect rockburst

Factors	Times (deep/total)	Effecting factors	Times (deep/total)
Bursting liability	150/289	Dip angle of coal seam	30/36
Mining depth	150/254	Advancing direction	19/24
Hard roof	150/235	Thickness of coal seam	10/15
Fault	132/184	Angle variation of coal seam	8/14
Fold	117/135	Insufficient protection measures	9/10
Disturbance (tunneling, drilling, and blasting, etc.)	98/102	Terminal line	8/8
Goaf management	40/81	Advancing speed	5/7
Coal pillar	34/63	Support patterns	5/6
Drift layout	22/54	Coal seam bifurcation, merger, pinch, etc.	2/2
Stability of coal seam	30/47	Gas	2/2
Hard floor	38/42	Planimetric feature	0/1
Overconcentrated mining activities	30/42	Floor water	1/1

literature and conducted a statistical analysis on factors resulting in rockburst. In view of the 300 rockburst accidents, the statistics of influencing factors related to rockburst are illustrated in Table 1.

By analyzing rockburst accidents, comparing those that occurred in deep and shallow coal seams, it was found that rockburst in the DCG is more likely accompanied by features of high-stress, large dip angle, hard thick roof, unstable coal seam, frequent and strong disturbances, unreasonable mining methods and insufficient protection measures. This may be due to the influence of the high original rock stress in deep mining (the gravity stress of rock is affected by the depth of mining and/or the residual tectonic stress is generated by geological structure), and a large amount of elastic strain energy is stored in the surrounding rock, which is sufficient to cause rockburst. In addition, the disturbance caused by mining activities such as, among others, blasting, reaming coal and driving will break the original balance of energies more easily and quickly. Moreover, the support patterns in roadways play a more crucial role in the DCG; that is, if the support is not adequate and cannot effectively offset the strain energy, dynamic disaster will be formed.

Optimization of CIM

The CIM is an early comprehensive evaluation method, which is widely applied to rockburst prediction before mining (Adoko et al. 2013; Shen et al. 2017). Based on previous investigation and analysis (Diederichs 2018) combined with the characteristics of the DCG, the geological and mining factors in the CIM were merged and inherited to optimize the

CIM. Seven geological factors were taken into account for the risk evaluation of rockburst, such as times of rockburst accidents, mining depth, hard thick roof, ratio of tectonic stress increment to normal stress, thickness characteristic of roof, uniaxial compressive strength of coal and elastic energy index. Eight mining factors affecting rockburst risk were considered, namely pressure relief degree of protective layer, thickness of reserve top/bottom coal, thickness of mining coal, width of working face in both sides of goaf, goaf treatment, horizontal distance between working face and coal pillar, distance between working face and fault and stress concentration factor.

To improve accuracy and applicability for risk evaluation of rockburst in DCG, this paper proposes six new evaluation indices, optimizes CIM and establishes the DCG-CIM. The corresponding evaluation system is elaborated in Figure 1.

Classification Basis for New Indicators

Dip Angle of Coal Seam

Field observation illustrates that the dip angle of coal seam has a great influence on the pressure of surrounding rock, especially in deep steep coal seams. Based on the geological situation of 2233 working face in the Hengda coal mine (see below), the influence of dip angle and rock pressure is analyzed preliminarily by means of a numerical simulation method. Three coal seam dip angles of 10°, 30° and 50° were selected, and the results are depicted in Figure 2.

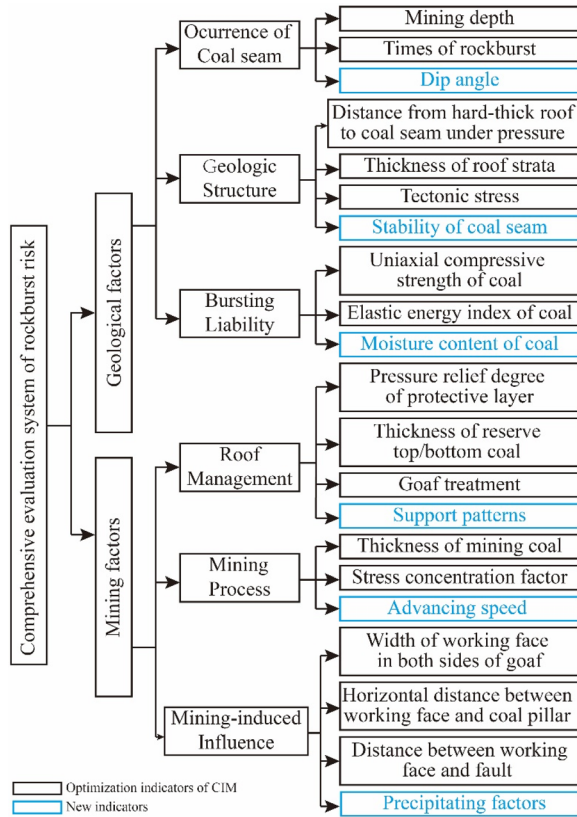


Figure 1. Comprehensive evaluation system of rockburst risk in the DCG.

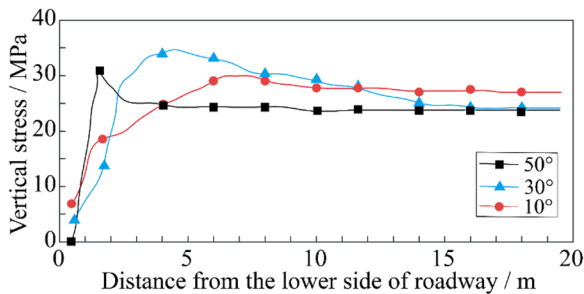


Figure 2. Change curves of stress state of coal mass of roadway before 65 m of open-off cut.

It was found that with increase in coal seam dip angle, the peak position of rock stress gradually moved close to the coal wall, the gradient of propensity stress gradually ascended and the range of the dynamic stress zone was constantly moving forward. This distributional and concentrated feature of stress in working face indicates that rockburst risk increases with dip angle of coal seam.

Therefore, this paper chose dip angle of coal seam (φ) as one of the indicators for risk evaluation of rockburst. The influencing degree is classified into four categories: (1) small influence: $\varphi < 8^\circ$, flat coal seam; (2) general influence: $8^\circ \leq \varphi \leq 25^\circ$, gently inclined coal seam; (3) moderate influence: $25^\circ \leq \varphi < 45^\circ$, inclined coal seam; and (4) strong influence: $\varphi \geq 45^\circ$, steep coal seam.

Stability of Coal Seam

In the DCG, due to increase in geo-stress, it is easy to form a strong unloading effect on the place where the thickness of the coal seam suddenly becomes bigger or smaller, which easily results in rockburst (Dou et al. 2012). When the thickness of a coal seam is locally thinned, the vertical geo-stress increases in the thin coal seam portion, and vice versa. The greater the thickness of a coal seam, the greater the stress concentration coefficient (Fig. 3). In addition, unstable coal seams with thinning areas, inclination variation region and bifurcation zone have a higher risk of rockburst; this situation is especially obvious in deep mining. The stability influence degree index R is defined as:

$$R = W_1 / W_2$$

where W_1 represents the increment of stress caused by the change of coal seam and W_2 represents the original rock stress of stable coal seam.

Therefore, the stability of coal seam is selected as one indicator to evaluate rockburst risk, and it is divided into four categories (Tang et al. 2010): (1) stability: small coal seam thickness change, coal seam without bifurcate, simple coal seam structure, $R < 1$; (2) general stability: general coal seam thickness change, not obvious bifurcation, general complex coal seam structure, $1 \leq R < 2$; (3) moderate stability: medium coal seam thickness change, obvious bifurcation, complex coal seam structure, $2 \leq R < 3$; and (4) instability: large coal seam thickness change, extremely obvious bifurcate, extremely complex coal seam structure, $3 \leq R$.

Moisture Content of Coal Seam

Water injection is one of the important measures to prevent rockburst in deep mining, because water can affect the strength, deformation and

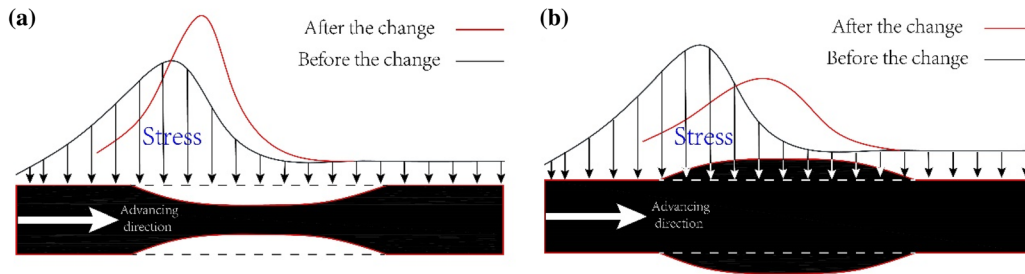


Figure 3. Schematic diagram of the stress distribution change of coal seam thickness: (a) thickness of coal seam becomes thinner, and (b) thickness of coal seam becomes thicker.

Table 2. Soaking Experimental Data of Coal Samples from the Changgouyu Coalmine

Coal sample	Soaking time	Samples size (diameter × height) (mm × mm)	Failure load (kN)	Compressive strength (MPa)
Rise race of the Changgouyu Coalmine	Natural moisture condition	50 × 100	49.95	25.47
	5 days	50 × 100	26.76	13.65
	10 days	50 × 100	24.39	12.44
	15 days	50 × 100	15.96	8.14

bursting liability of coal–rock mass (Liu et al. 2018). Through the soaking experiment of standard coal samples from the Changgouyu Coalmine at different time, the obtained results are shown in Table 2.

As far as the results are concerned, due to the decrease in strength of coal after water injection, the deformation characteristics become “plasticized”. This means that the ability of coal to accumulate elastic energy decreases and the ability to consume elastic energy by plastic deformation increases, resulting in a significant decrease in the bursting liability of coal after water injection or even complete loss. This phenomenon is particularly evident in deep mining (Liu et al. 2017).

However, the moisture content of the coal sample in the laboratory is different from the natural state of the coal seam, and the bursting liability indices in the CIM cannot really and exactly reflect the influence of moisture content on the potential risk of rockburst. Therefore, it is essential to use moisture content (ω) as a separate index to evaluate rockburst risk. Mao et al. (2001) analyzed widely the bursting liability of different coal seams in more than ten deep coalmines in the Xuzhou and Datun ore districts. They found that the original moisture content of coal with bursting liability was generally around 1.5%. When moisture content increased by

1–2%, the bursting liability was reduced dramatically. Therefore, in this paper, the influencing degree of moisture content on rockburst was classified preliminarily into four categories: (1) strong influence: $\omega < 1.5\%$; (2) moderate influence: $1.5\% \leq \omega \leq 3\%$; (3) general influence: $3\% \leq \omega \leq 5\%$; and (4) small influence: $\omega > 5\%$.

Advancing Speed of Working Face

Under the situation of DCG, the advancing speed of working face is bound up with the scale of the energy release and frequency of rockburst. With the model established above (in section Dip Angle of Coal Seam), FLAC3D was applied to analyze the influence of the advancing speed of working face (specified at 2 m/d, 4 m/d, 6 m/d and 8 m/d) on stress and displacement (Fig. 4). The simulation results show that properly accelerating the advancing speed of the working face can reduce the remaining time of the working face at the same position and maintain better the stability of the roadway. However, with development of the advancing speed of working face, the high-stress area of the coal body approaches the working face; besides, the excessive accumulation of elastic energy may lead to rock-

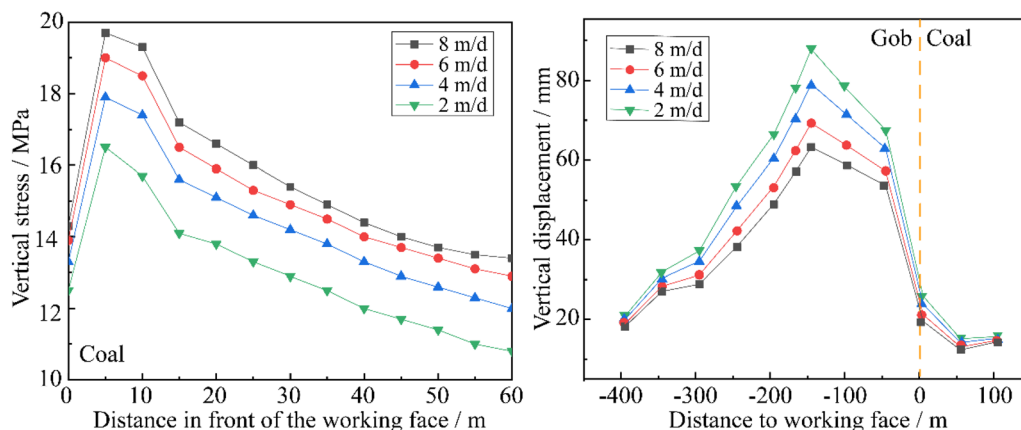


Figure 4. Stress and displacement curves at different advancing speeds.

burst. In general, the fastest advancing speed of working face cannot exceed 4 m/d in rockburst coalmine (Feng et al. 2012). However, the optimal advancing speed of working face should be selected based on the actual situation.

In view of the general situation of rockburst coalmines, the advancing speed of working face (v) is classified into three categories in this paper: (1) reasonable: uniform velocity, $1 \text{ m/day} < v < 3 \text{ m/day}$; (2) generally reasonable: no sudden sharp change, $3 \text{ m/day} < v < 4 \text{ m/day}$ or $v < 1 \text{ m/day}$; and (3) unreasonable: $4 \text{ m/day} < v$ and the speed of rapid change. The evaluation index of the advancing speed of working face varies according to mining conditions in different mines. The specific calculation process can be obtained from Dou and He (2001).

Precipitating Factors

In the DCG, there are abundant precipitating factors that can break the stress balance of coal–rock, such as, among others, blasting, reaming coal, first weighting, periodic weighting, driving and “square” (when the mining length of the working face is equal to the width of the working face, we call it “square” or “one times square”; when the mining length is twice the width, it is called “two times square”). These factors can locally change the stress state of the coal–rock. On the one hand, the stress in the coal seam rapidly redistributes and promptly increases the intensity of rock pressure; on the other hand, the lateral restraint resistance of the coal seam

edge can be quickly removed, which could reduce the compressive strength and cause rapid destruction of coal–rock mass. For example, a rockburst accident in the Beijing Mentougou mine caused directly by blasting accounted for 78%; in the Fushun Longfeng Coalmine, more than half of rockburst accidents took place during the process of periodic weighting and many times square (Li et al. 2007; Zhou et al. 2016). Therefore, the degree of precipitating factors (P) induced is defined as:

$$P = (\max \{ \sigma_{d1}, \sigma_{d2}, \sigma_{d3} \dots \sigma_{dn} \} \times \lambda + \sigma_s / \sigma_{bmin})$$

where σ_s refers to the static stress within the coal–rock mass, σ_d refers to the dynamic stress induced by precipitating factors, λ refers to the pre-disposition coefficient, which is the total number of precipitating factors divided by the number of times the average intensity is exceeded, and σ_{bmin} refers to the critical stress required for a rockburst to occur (all in MPa). When the rock pressure appears to be high stress concentration, the probability and risk of rockburst will increase. In this paper, the precipitating factor P was chosen as one indicator for the risk evaluation of rockburst, and it is divided into three categories: (1) small: $P < 0.5$; (2) general: $0.5 \leq P < 1$; and (3) strong: $1 \leq P$.

Support Patterns in Roadways

Thanks to the scientific and reasonable support of the deep mine roadways, which help improve the overall strength and residual strength of the surrounding rock with high effectiveness, the bearing

capacity can still be effective even though the coal-rock is destroyed, and the support can continue to control the recurrence of rockburst. At present, there are many support patterns applied in roadways, such as, among others, shotcrete, I-shape rigid support, H-shape steel yielding support, U-shape steel yielding support, bolt, anchor, anchor beam web, truss bolts, anchor spraying, bolting-grouting, and high-strength concrete arc plate support. U-shape steel yielding support and bolt support (including plastic mesh, metal mesh, shotcrete, W-shaped steel strip, steel ladder beam or the combined form of trusses) is the most important support technology (Hoke et al. 2000).

When installed and equipped with different support patterns, there is a distinct variety of impact on rockburst strength for the coal-rock mass. In this paper, the support patterns were selected as evaluation indicators for rockburst, and they are divided into three categories: (1) good: the joint support is adopted by various support methods; (2) general: a single shrinkable support method (such as a bolt) or the rigid support (such as the wooden shed bracket and the I-shaped steel bracket) is used; and (3) poor: no support in roadway.

Establishment of DCG-CIM

As an improved evaluation method for deep mining, the flowchart of the DCG-CIM is shown in Figure 5.

To begin with, the evaluation zone is divided into different levels of potentially dangerous areas based on factors of the DCG-CIM such as, among others, surrounding goaf, upper and lower coal seams, coal pillar and first weighting. After the potentially dangerous areas are evaluated using the DCG-CIM, the evaluation results can be divided into four risk grades [no rockburst risk (*N*), weak rockburst risk (*W*), medium rockburst risk (*M*) and strong rockburst risk (*S*)]. Next, the superposition principle of “Same levels, risk upgrade; Different levels, select the maximum” is adopted to obtain accurate and detailed grading diagram of rockburst risk in the evaluation zone. Eventually, combined with the evaluation results of geological and mining technical conditions, the risk superposition calculation is carried out for each zone of the working face. The specific risk-grades evaluation standards and principle are elaborated in Tables 3 and 4.

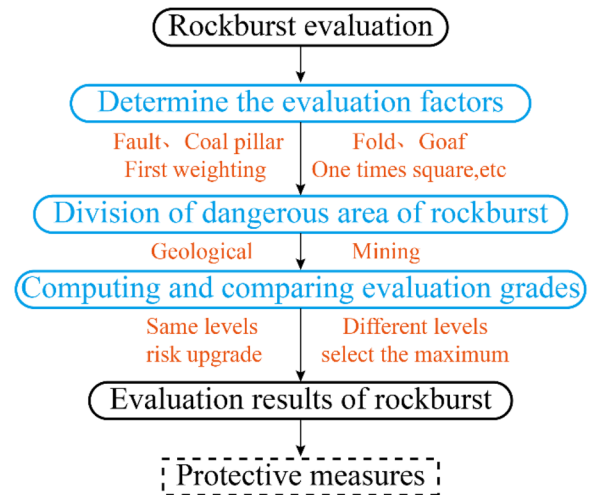


Figure 5. Evaluation flowchart of DCG-CIM.

APPLICATION OF DCG-CIM

In this paper, the DCG-CIM was applied to many rockburst coalmines such as, among others, the Hengda Coalmine, Qianqiu Coalmine, Changyugou Coalmine and Nanshan Coalmine. The evaluation results show that the DCG-CIM can accurately and effectively predict the rockburst risk zone. Due to space limitations, this paper takes the Hengda Coalmine, which has recently suffered a rockburst accident, as an example to verify the correctness of the DCG-CIM.

The Hengda Coalmine

The Hengda Coalmine owns six coal seams, located in Fuxin City, Liaoning Province, China. This study chose 2233 working face in the 126-mining area (Sunjiawan No. 1 coal seam). The burial depth of this coal seam was about 900–980 m, its average thickness was 5 m and its dip angle was 7°. The geological conditions are shown in Figure 6.

The roof of the 2233 working face was glutenite, which is relatively thick and hard. It adopted the inclined mining method and the mining area was 700 m × 200 m. The north of the working face was 2132 and 2232 goafs, the original coal mass on the south, the 126-mining area uphill system to the west and the Ping'an No. 2 fault to the east. The lower part was original coal mass, and the top was 1363

Table 3. Geological factors

Number	Evaluation indicator	Explanation	Classification	Evaluation index
1	W_1	History of rockburst in the same level coal seam (times/ N)	$N = 0$	0
			$N = 1$	1
			2–3	2
			$N \geq 3$	3
2	W_2	Mining depth (H)	$H \leq 400$ m	0
			400–600 m	1
			600–800 m	2
			$H > 800$ m	3
3	W_3	Distance between hard thick roof and coal seam when pressure is not relieved (D)	$D > 100$ m	0
			50–100 m	1
			20–50 m	2
			$D \leq 20$ m	3
4	W_4	Ratio of tectonic stress increment to normal stress in mining area ($\gamma = (\sigma_g - \sigma) / \sigma$)	$\gamma \leq 10\%$	0
			10–20%	1
			20–30%	2
			$\gamma > 30\%$	3
5	W_5	Characteristic parameters of roof strata thickness (L_{st})	$L_{st} < 50$ m	0
			50–70 m	1
			70–90 m	2
			$L_{st} > 90$ m	3
6	W_6	Uniaxial compressive strength of coal (R_c)	$R_c \leq 7$ MPa	0
			7–10 MPa	1
			10–14 MPa	2
			$R_c > 14$ MPa	3
7	W_7	Elastic energy index of coal (W_{ET})	$W_{ET} < 2$	0
			$2 \leq W_{ET} < 3.5$	1
			$3.5 \leq W_{ET} < 5$	2
			$W_{ET} \geq 5$	3
8	W_8	Moisture content of coal seam (ω)	$\omega \geq 5\%$	0
			$3\% \leq \omega < 5\%$	1
			$1.5\% \leq \omega < 3\%$	2
			$\omega < 1.5\%$	3
9	W_9	Dip angle of coal seam (φ)	$\varphi < 8^\circ$	0
			$8^\circ \leq \varphi < 25^\circ$	1
			$25^\circ \leq \varphi < 45^\circ$	2
			$45^\circ < \varphi$	3
10	W_{10}	Stability of coal seam (coefficient/ R)	$R < 1$	0
			1–2	1
			2–3	2
			$R \geq 3$	3
Risk grades	$W_{rl} = \frac{\sum_{i=1}^n W_i}{\sum_{i=1}^n W_{imax}}$		$W_{rl} \leq 0.25$	N
			$0.25 < W_{rl} \leq 0.5$	W
			$0.5 < W_{rl} \leq 0.75$	M
			$W_{rl} > 0.75$	S

Table 4. Mining factors

Number	Evaluation indicator	Explanation	Classification	Evaluation index
1	W_1	Pressure relief degree of protective layer	Good	-4
			Moderate	2
			Worse	4
2	W_2	Thickness of reserve top/bottom coal (H_{tb})	<0.5 m	0
			0.5–1 m	1
			≥ 1 m	3
3	W_3	Thickness of mining coal seam under pressure (H_t)	<3.0 m	0
			3.0–4.0 m	1
			>4.0 m	2
4	W_4	Width of working face in both sides of goaf (L_{bi})	>300 m	0
			150–300 m	2
			<150 m	3
5	W_5	Goaf treatment	Filling method	0
			Caving method	2
6	W_6	Horizontal distance between working face or roadway and coal pillar, which is left over from upper protective layer after mining (H_z)	>60 m	0
			30–60 m	2
			<30 m	4
7	W_7	Distance between working face and fault (drop is greater than 3 m) (L_d)	≥ 200 m	0
			50–200 m	1
			<50 m	2
8	W_8	Stress concentration factor (K)	<1	0
			1–2	3
			>2	4
9	W_9	Support patterns	Combined support	0
			Single yielding support/rigid support	1
			No support	2
10	W_{10}	Advancing speed	3 m/d > $v \geq 1$ m/d	0
			4 m/d > $v \geq 3$ m/d or 1 m/d > v	1
			$v \geq 4$ m/d	2
11	W_{11}	Precipitating factors (coefficient/ P)	$0.5 > P$	0
			$1 > P \geq 0.5$	3
			$P \geq 1$	4
			$W_{r2} \leq 0.25$	N
Risk grades	$W_{r2} = \frac{\sum_{i=1}^n W_i}{\sum_{i=1}^n W_{imax}}$		$0.25 < W_{r2} \leq 0.5$	W
			$0.5 < W_{r2} \leq 0.75$	M
			$W_{r2} > 0.75$	S

goaf and 1362 working face in the Sunjiawan No. 2 coal seam; the average thickness of the coal seam was 4 m. Many microseismic phenomena were recorded in the mining process, mainly due to the stress disturbances caused by, among others, blasting and driving.

Division of Potentially Dangerous Areas

Based on previous investigations and statistical analyses of rockburst accidents, it was found that the rockburst happens usually in the ventilation road-

way, the haulage roadway and the open-off cut area. To analyze the influence of periodic weighting, square and other disturbance phenomena on rockburst, the interval of periodic weighting of the 2233 working face was set about 30 m, and the scope of 30 m before and after “square” was considered as the potentially dangerous area by observing the intensity of rock pressure on the same coal seam. To this end, the potentially dangerous areas were divided using the DCG–CIM. The classification criteria are shown in Tables 5, 6, 7, and 8. The results are shown in Figure 7.

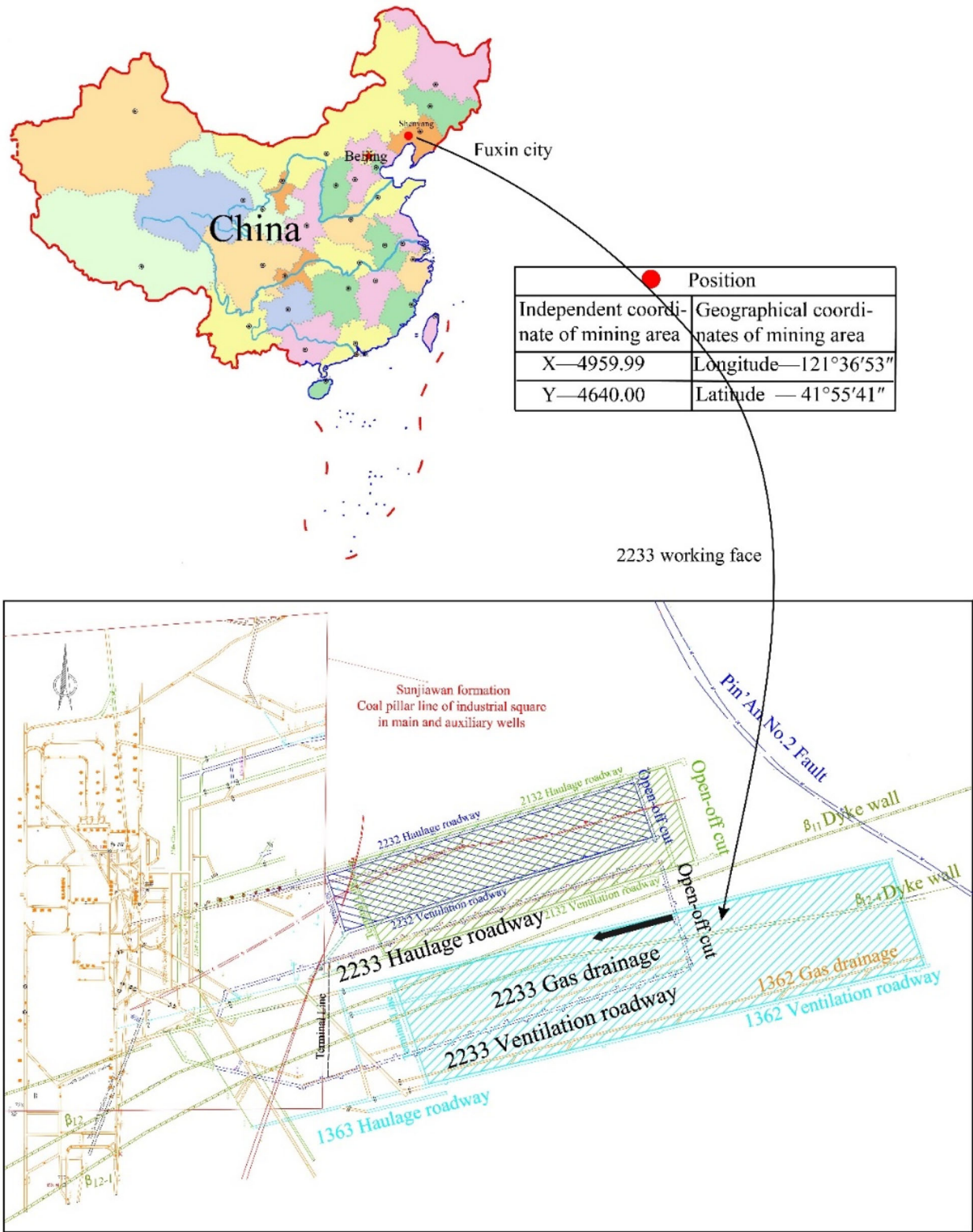


Figure 6. Geological information of the Hengda Coalmine and layout of the 2233 working face.

Table 5. Division interval of ventilation roadway in the 2233 working face

Name ^a	Interval (m)	Length (m)	Major influencing factors
H1	0–162	162	1362 coal pillar, W_{10} fault
H2	162–449	287	1362 coal pillar
H3	449–579	130	Completely liberated area
H4	579–844	265	Liberated area, retain coal thickness greater than 1 m
H5	844–903	59	Completely liberated area

^aH is interval of ventilation roadway

Table 6. Division interval of haulage roadway for the 2233 working face

Name ^a	Interval (m)	Length (m)	Major influencing factors
Y1	0–48	48	2232 coal pillar
Y2	48–332	284	2232 and 2132 coal pillar
Y3	332–869	537	Completely liberated area

^aY is interval of haulage roadway

Risk Assessment and Analysis of Geological Factors

The bursting liability of coal–rock is the internal cause and necessary condition for inducing rockburst, but not all rock-coal mass with bursting liability will result in rockburst. It is also related to other geological environmental factors, which can provide in situ stress conditions for the coal–rock. According to the geological conditions of the 2233 working face, the evaluation index of rockburst can be confirmed, and then the risk grades of rockburst can be calculated. The evaluation results of the overall geological factors of the coal seam at the 2233 working face are shown in Table 9.

From Table 9, the 2233 working face belongs to weak rockburst risk zone according to the results of the evaluation index ($W_{r1} = 0.433$) and needs further evaluation and treatment with the help of involving mining factors.

Risk Evaluation and Analysis of Mining Factors

Before starting mining activities, the coal–rock mass is in a natural equilibrium state of stress (Jiang et al. 2014; Wang et al. 2019; Feng et al. 2020). When the stope or/and roadways are excavated, the original rock stress is redisturbed and the secondary stress (mining stress) is generated in the surrounding

rock. The mining stress could be superimposed on the original rock stress in the process of mining in different areas, which is easy to generate a high stress concentration of coal–rock mass and increase the potential risk of rockburst. According to the mining conditions of the 2233 working face, the evaluation index of rockburst can be determined and then the risk grades of rockburst can be calculated. The evaluation results of each section of the 2233 working face are shown in Table 10.

The results determined by mining factors (Table 10) show the following. H-1 ($W_{r2} = 0.53$) and H-2 ($W_{r2} = 0.56$) are medium rockburst risk zones. H-3 ($W_{r2} = 0.09$), H-4 ($W_{r2} = 0.19$) and H-5 ($W_{r2} = 0.12$) are no rockburst risk zones. Y-1 ($W_{r2} = 0.53$) and Y-2 ($W_{r2} = 0.59$) are medium rockburst risk zones and Y-3 ($W_{r2} = 0.25$) is a no rockburst risk zone. Q1 ($W_{r2} = 0.56$) is medium rockburst risk zone, but Q2 ($W_{r2} = 0.09$) is no rockburst risk zone. YPS1/HPS1 ($W_{r2} = 0.5$), YPA2/HPA2 ($W_{r2} = 0.5$), YPS3/HPS3 ($W_{r2} = 0.4$), YPA4/HPA4 ($W_{r2} = 0.4$) and YP5/HP5 ($W_{r2} = 0.4$) are weak rockburst risk zones.

Evaluation Results of DCG–CIM

Based on the above results, the locations and risk grades of the potentially dangerous areas were determined by applying the coupling superposition principle. According to the evaluation system, each zone can be divided into four types regarding the potentially dangerous degree. The sketch map (Fig. 8) presents the risk grades of rockburst according to Tables 9 and 10.

The 2233 ventilation roadway, close to the W_{10} fault, is affected by high stress concentration due to the left coal pillar surrounding the 1362 goaf. Considering the geological conditions in the weak

Table 7. Division interval of open-off cut of the 2233 working face

Name ^a	Interval (m)	Length (m)	Major influencing factors
Q1	0–121	121	Coal pill between the 1362 haulage roadway and 2132 ventilation roadway
Q2	121–200	79	Completely liberated area

^aQ is interval of open-off cut

Table 8. Division interval of disturbance factors on the 2233 working face

Name ^a	Interval (m)	Length (m)	Major influencing factors
YPS1/HPS1	473–533	60	Two times square and periodic weighting
YPA2/HPA2	573–633	60	Periodic weighting and square
YPS3/HPS3	673–733	60	Square and periodic weighting
YPA4/HPA4	773–833	60	Periodic weighting and square
YP5/HP5	843–873	30	First weighting

^aYPS, HPS, YPA denote the interval of disturbance factors

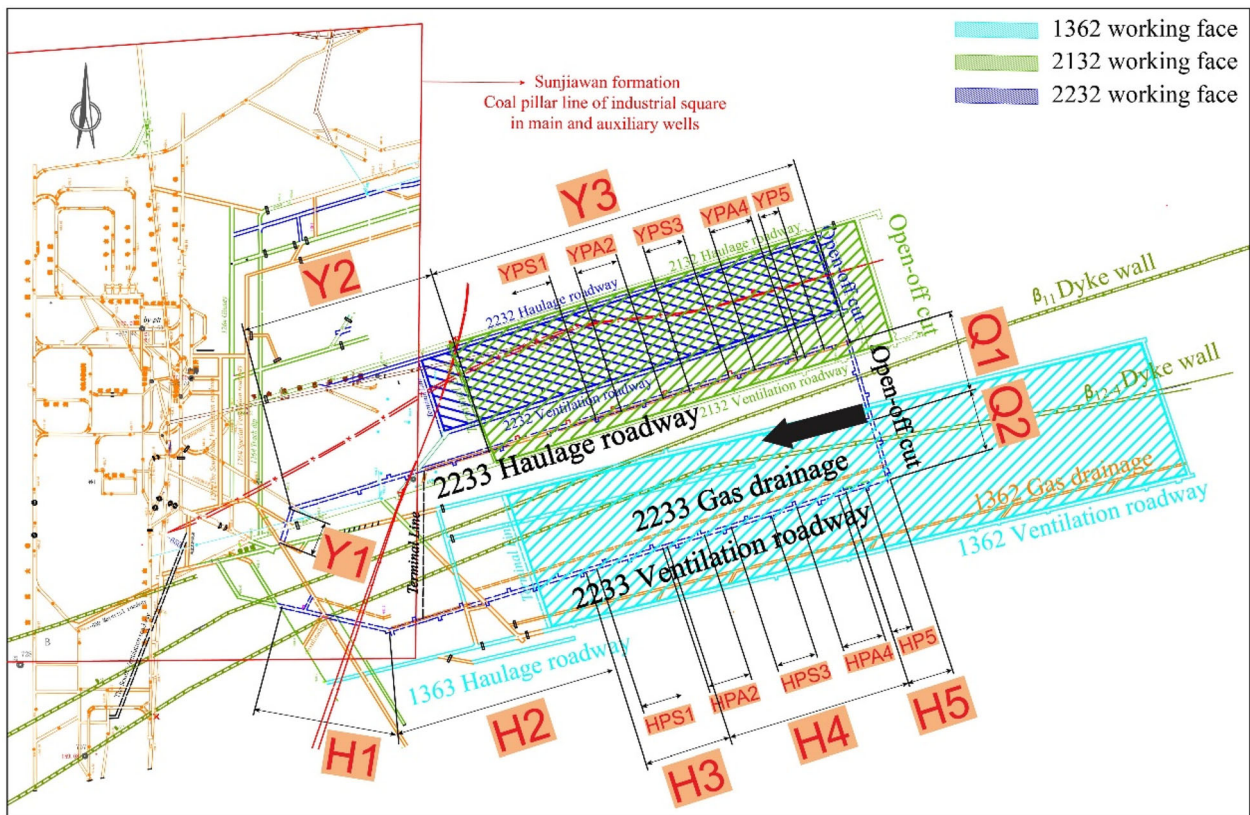


Figure 7. Schematic diagram of classification of potentially dangerous areas.

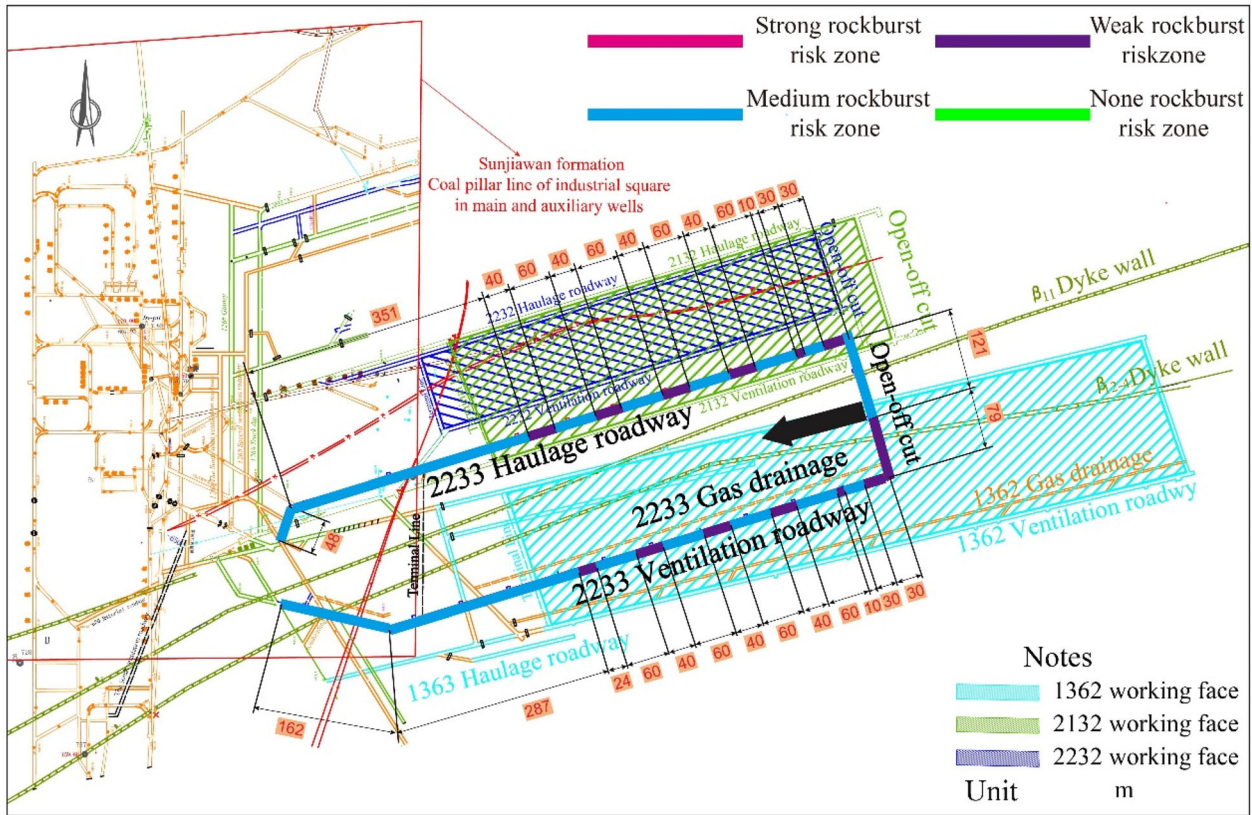


Figure 8. Classification of risk grades in the 2233 working face.

rockburst risk zone, and following the principle of superposition, the medium rockburst risk zone was determined in the ranges of 0–184 m, 224–284 m, 324–384 m, 424–484 m, 524–584 m and 594–624 m from the terminal line, and the rest was weak rockburst risk zone. The open-off cut close to the haulage roadway with a length about 121 m was identified as the medium rockburst risk zone. Although the open-off cut was located within the completely liberated area, this sector was influenced by the coal pillars in the 2232 goaf in the north side and the concentrated stress as a result of the coal pillars in the upper goaf 2132, 1362. The remaining part was deemed as weak rockburst risk zone; the north side of the haulage roadway shared coal pillars with the 2232 goaf, which was also located in the influence range of the 2132 goaf. Blasting, mining and other factors have a significant impact on the occurrence of rockburst in this area. Therefore, the medium rockburst risk area of haulage roadway was within the ranges of 0–184 m, 224–284 m, 324–384 m, 424–484 m, 524–584 m and 594–624 m inside

the terminal line, and the rest was weak rockburst risk zone.

DISCUSSION

Case Study

On August 6, 2018, rockburst suddenly took place in the 2233 working face of the 126-mining area. The scope of this rockburst was wide, and the broken region was scattered in multiple sections. The haulage roadway in the ranges of 150–180 m has been seriously damaged, mainly including the 15 m range of 143–158 m, the 58 m range of 223–281 m and the 15 m range of 326–341 m in the terminal line (Fig. 9).

The preliminary analysis of rockburst was as follows. Under the combined effect of deep burial depth, complex stope structure and dense roadways, the result was that the rock seam of roof above the 2233 working face bore too much pressure, while the

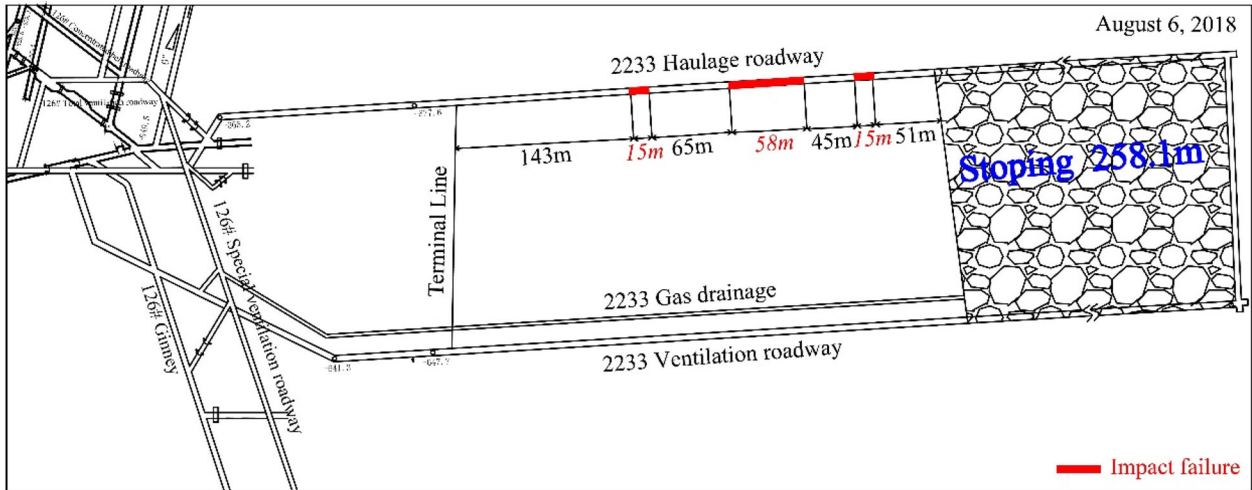


Figure 9. Schematic diagram of impact failure area of the 2233 working face.

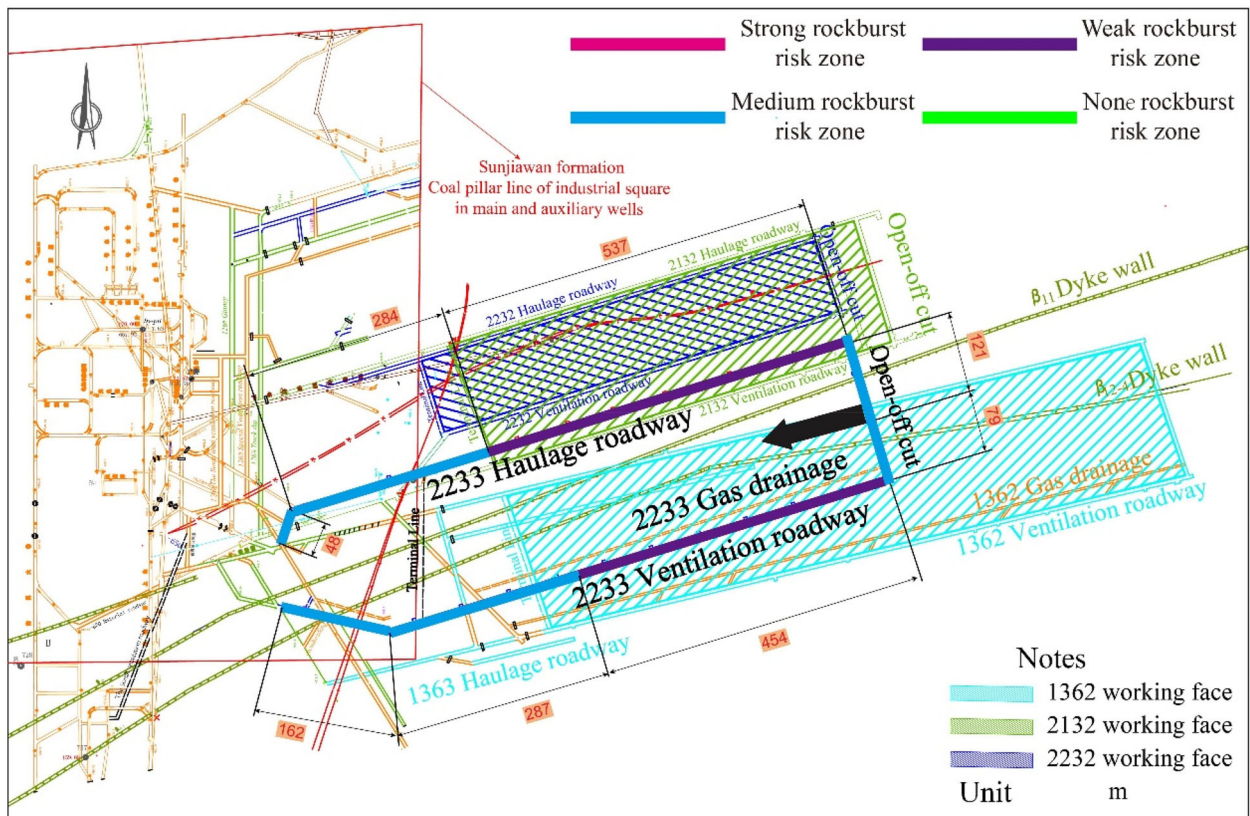


Figure 10. Schematic diagram of classification of rockburst risk grades based on the CIM.

Table 9. Geological factor evaluation results on 2233 working face

Number	Evaluation indicator	Explanation	W_i
1	W_1	$N = 0$	0
2	W_2	$H = 900 \text{ m} > 800 \text{ m}$	3
3	W_3	$D = 263 \text{ m} > 100 \text{ m}$	0
4	W_4	$10\% < \gamma = 16.33\% < 20\%$	1
5	W_5	$L_{st} = 92.17435 > 50$	3
6	W_6	$7 \text{ MPa} < R_c = 8.32 \text{ MPa} < 10 \text{ MPa}$	1
7	W_7	$2 < W_{ET} = 3.056 < 3.5$	1
8	W_9	$1.5\% < \omega = 2.3\% < 3\%$	2
9	W_{10}	$\varphi = 7^\circ < 8^\circ$	0
10	W_{11}	$R = 2$	2

direct roof was firm and did not collapse, concentrating excessive stress and resulting in rockburst. Comparing the rockburst risk zone in Figures 8 and 9, the medium rockburst risk zone delineated with the DCG–CIM completely covered the actual area of rockburst, which demonstrates that the DCG–CIM can accurately and effectively predict the scope and risk grades of rockburst.

CIM and DCG–CIM

CIM is a common evaluation method for analyzing rockburst risk. According to the mining and geological conditions, the risk grades of rockburst were obtained using the CIM (Fig. 10). The evaluation results show that the medium rockburst risk zone of the haulage roadway was within 117 m of the terminal line and the rest was weak rockburst risk zone. The whole segment of the open-off cut was medium rockburst risk zone. In the ventilation roadway, it was within 200 m from the terminal line and the rest was weak rockburst risk zone.

Comparing Figures 9 and 10, the rockburst risk zone evaluated was near the actual damage area, but the coincidence degree was poor, less than 80%. By comparing Figures 8, 9 and 10, it was found that the evaluation result of the two methods was quite different, and the DCG–CIM had greater advantages in evaluating the DCG. For example, within the range of 143–158 m from the terminal line, with DCG–CIM, it was considered to be a medium rockburst risk zone but, with CIM, it was considered it to be a weak rockburst risk area. In the range of 79 m from the open-off cut to ventilation roadway, it was considered to be a weak rockburst risk zone

with the DCG–CIM, while it meets the risk grades of being a medium rockburst risk zone with the CIM.

Follow-Up Prevention Suggestions

1. According to the evaluation results of the DCG–CIM, combined with the mining length of the working face, the area of the rockburst prevention and control should be expanded appropriately and the support needs to be strengthened.
2. According to the risk grades of each zone divided with the DCG appropriately CIM, protective measures should be taken: for example, coal seam water injection, large-diameter drilling, goaf backfilling, roadway support, roof loosening through preblasting and other measures to reduce, transfer and offset stress concentration, release energy in advance, thereby to control rockburst risk (Huang et al. 2015; Liu et al. 2017; Li et al. 2019).
3. In addition, EMR and AE monitoring data analysis and early warning should be strengthened (Wang et al. 2005; Song et al. 2018). During mining, due to the nonuniformity of roof and the changing of high-level roof and stope structure, making the process of redistribution, transfer, agglomeration and release on rock pressure is quite complicated. It is recommended to install a mine microseismic monitoring system to detect roof activity at all place. The trend method and the key point monitoring method should be combined to analyze the early warning

Table 10. Mining factors evaluation results for the 2233 working face

Number	Evaluation indicator	Explanation	Y1	Y2	Y3	H1	H2	H3	H4	H5	Q1	Q2	YPS1/HPS1	YPA2/HPA2	YPS3/HPS3	YPA4/HPA4	YPS5/HP5
1	W ₁	Pressure relief degree	4	4	-4	4	4	-4	-4	-4	4	-4	2	2	2	2	2
2	W ₂	H _{lb}	0	0	0	0	0	0	3	0	0	0	0	0	0	0	0
3	W ₃	H _l	0	0	0	0	0	0	0	0	0	0	0	0	0	0	0
4	W ₄	L _{bi}	0	0	0	0	0	0	0	0	0	0	0	0	0	0	0
5	W ₅	Goaf treatment	2	2	2	2	2	2	2	2	2	2	2	2	2	2	2
6	W ₆	H _z	4	4	4	4	4	0	0	0	4	0	4	4	4	4	4
7	W ₇	L _{ld}	0	0	0	0	0	0	0	0	0	0	0	0	0	0	0
8	W ₈	K	3	4	0	3	4	0	0	0	3	0	3	3	0	0	0
9	W ₉	Support patterns	0	0	0	0	0	0	0	0	0	0	0	0	0	0	0
10	W ₁₀	Advancing speed	1	1	2	1	1	1	1	2	2	2	1	1	1	1	2
11	W ₁₁	Precipitating factors	3	4	4	3	3	4	4	4	3	3	4	4	4	4	3
12	W ₁₂	Risk grades	0.53	0.59	0.25	0.53	0.56	0.09	0.19	0.12	0.56	0.09	0.5	0.5	0.4	0.4	0.4
13			M	M	N	M	M	N	N	N	M	N	W	W	W	W	W

Factors: H is interval of ventilation roadway. Y is interval of haulage roadway. Q is interval of open-off cut. YPS, HPS, YPA denote the interval of disturbance factors. Risk grades: M = moderate, N = no risk, W = weak

data. When the analysis system finds an abnormality, the appropriate prevention measures should be taken. Particularly, when rockburst risk is beyond the threshold of security, miners should be evacuated immediately.

CONCLUSIONS

In this paper, the DCG-CIM was proposed for evaluating rockburst risk in the DCG. With the “8·6” rockburst accident in the Hengda Coalmine, the rationality and correctness of the six new evaluation indices and the accuracy and effectiveness of the DCG-CIM were tested and verified. The prevention and control suggestions for rockburst were conducted on the basis of evaluation results. The study attained mainly the following conclusions:

1. For DCG, based on previous studies, this paper summarized several field cases, put forward six new evaluation indices and made a detailed analysis. The results show that rockburst risk increases with increase in dip angle, advancing speed of working face and precipitating factors, and with decrease in moisture content, support patterns and the stability of coal seam.
2. In this paper, based on the geological condition of DCG, the existing method was improved, and combined with the six newly proposed indices, the DCG-CIM was established to realize accurate and efficient assessment of rockburst risk. Compared with the traditional methods, the DCG-CIM is more suitable for DCG, which is of great significance for mine safety production.
3. Combined with the “8·6” rockburst accident of the 2233 working face in the Hengda Coalmine, the evaluation results of DCG-CIM are the following. The dangerous area of the haulage roadway was within the range of 84 m from 0 to 84 m from the terminal line, 60 m in the range of 224–284 m, 60 m in the range of 324–384 m, and 60 m in the range of 424–484 m. Within the range of 60 m in the range of 524–584 m and 30 m in the range of 594–624 m, the predicted areas of rockburst using the DCG-CIM completely covered the actual area of rockburst.

ACKNOWLEDGMENTS

This research was funded by the Future Scientists Program of “Double First Class” of China University of Mining and Technology (2019WLKXJ061), the National Natural Science Foundation of China (No. 51934007), the National Natural Science Foundation of China (No. 51934007, 52004267), the National Science Foundation for Young Scientists of Jiangsu Province (BK20180644).

REFERENCES

- Adoko, A. C., Gokceoglu, C., Wu, L., & Zuo, Q. J. (2013). Knowledge-based and data-driven fuzzy modeling for rock burst prediction. *International Journal of Rock Mechanics and Mining Sciences*, 61, 86–95.
- Afraei, S., Shahriar, K., & Madani, S. H. (2018). Statistical assessment of rock burst potential and contributions of considered predictor variables in the task. *Tunnelling and Underground Space Technology*, 72, 250–271.
- Bräuner, G. (2017). *Rock bursts in coal mines and their prevention*. London: Routledge.
- Cai, W., Dou, L., Zhang, M., Cao, W., Shi, J. Q., & Feng, L. (2018). A fuzzy comprehensive evaluation methodology for rock burst forecasting using microseismic monitoring. *Tunnelling and Underground Space Technology*, 80, 232–245.
- Cheng, Z., Liu, B., Zou, Q., Wang, X., Feng, J., Zhao, Z., & Sun, F. (2020). Analysis of spatial-temporal evolution of mining-induced fracture field: A case study using image processing in the Shaqu coal mine, China. *Natural Resources Research*, 29(3), 1601–1615.
- Dou, L. M., & He, X. Q. (2001). *Theory and technology of rock burst prevention* (pp. 35–39). Xuzhou: China University of Mining and Technology Press.
- Dou, L. M., & He, X. Q. (2004). Model for rock burst failure and its critical values of acoustic and electromagnetic emission. *Journal-China University of Mining and Technology (Chinese edition)*, 33, 504–508.
- Dou, L., Chen, T., Gong, S., He, H., & Zhang, S. (2012). Rock burst hazard determination by using computed tomography technology in deep workplace. *Safety Science*, 50, 736–740.
- Diederichs, M. S. (2018). Early assessment of dynamic rupture hazard for rockburst risk management in deep tunnel projects. *Journal of the Southern African Institute of Mining and Metallurgy*, 118(3), 193–204.
- Feng, X. T., Xiao, Y. S., & Feng, G. L. (2012). Mechanism, warning and dynamic control of rock burst evolution process. In: *ISRM Regional Symposium-7th Asian Rock Mechanics Symposium*. International Society for Rock Mechanics and Rock Engineering.
- Feng, X., & Zhang, Q. (2018). The effect of backfilling materials on the deformation of coal and rock strata containing multiple goaf: A numerical study. *Minerals*, 8, 224.
- Feng, X., Zhang, Q., Wang, E., Ali, M., & Zhang, G. (2020). 3d modeling of the influence of a splay fault on controlling the propagation of nonlinear stress waves induced by blast loading. *Soil Dynamics and Earthquake Engineering*, 138, 106335.
- Hoek, E., Kaiser, P. K., & Bawden, W. F. (2000). *Support of underground excavations in hard rock*. Boca Raton: CRC Press.
- He, X., Chen, W., Nie, B., & Zhang, M. (2010). Classification technique for danger classes of coal and gas outburst in deep coal mines. *Safety Science*, 48, 173–178.
- He, M., Zhao, F., Cai, M., & Du, S. (2015). A novel experimental technique to simulate pillar burst in laboratory. *Rock Mechanics and Rock Engineering*, 48, 1833–1848.
- Huang, B., Wang, Y., & Cao, S. (2015). Cavability control by hydraulic fracturing for top coal caving in hard thick coal seams. *International Journal of Rock Mechanics and Mining Sciences*, 74, 45–57.
- He, J., Dou, L., Gong, S., Li, J., & Ma, Z. (2017). Rock burst assessment and prediction by dynamic and static stress analysis based on micro-seismic monitoring. *International Journal of Rock Mechanics and Mining Sciences*, 100, 46–53.
- Hussain, R., & Luo, K. (2020). Geochemical evaluation of enrichment of rare-earth and critical elements in coal wastes from Jurassic and Permo-carboniferous coals in Ordos Basin, China. *Natural Resources Research*, 29, 1731–1754.
- Jiang, F., Feng, Y., & Liu, Y. (2014). Dynamic evaluation method for rock burst risk before stopping. *Chinese Journal of Rock Mechanics and Engineering*, 33, 2101–2106.
- Kong, X., Wang, E., Li, S., Lin, H., & Ju, Y. (2019). Dynamic mechanical characteristics and fracture mechanism of gas-bearing coal based on SHPB experiments. *Theoretical and Applied Fracture Mechanics*, 105, 102395.
- Li, T., Cai, M., & Cai, M. (2007). A review of mining-induced seismicity in China. *International Journal of Rock Mechanics and Mining Sciences*, 44, 1149–1171.
- Li, X., Wang, E., Li, Z., Liu, Z., Song, D., & Qiu, L. (2016). Rock burst monitoring by integrated micro-seismic and electromagnetic radiation methods. *Rock Mechanics and Rock Engineering*, 49, 4393–4406.
- Liu, X., Xu, G., Zhang, C., Kong, B., Qian, J., Zhu, D., & Wei, M. (2017). Time effect of water injection on the mechanical properties of coal and its application in rock burst prevention in mining. *Energies*, 10(11), 1783.
- Liu, X., & Wang, E. (2018). Study on characteristics of EMR signals induced from fracture of rock samples and their application in rock burst prediction in copper mine. *Journal of Geophysics and Engineering*, 15, 909–920.
- Li, Z. L., He, X. Q., Dou, L. M., & Song, D. Z. (2018). Comparison of rock burst occurrence during extraction of thick coal seams using top-coal caving versus slicing mining methods. *Canadian Geotechnical Journal*, 55, 1433–1450.
- Liu, Z., Cao, A., Guo, X., & Li, J. (2018). Deep-hole water injection technology of strong impact tendency coal seam—a case study in Tangkou coal mine. *Arabian Journal of Geosciences*, 11, 12.
- Li, M., Zhang, J., An, B., Germain, D., & Xu, Q. (2019). Effect of cyclic lateral loading on the compaction behaviour of waste rock backfill materials in coal mines. *Energies*, 12(1), 17.
- Mao, X., Chen, Z., Xu, S., & Li, T. (2001). Experimental study on the relation between the burst tendency and water content in coal seam. *Chinese Journal of Rock Mechanics and Engineering*, 20, 49–52.
- Pan, Y. S., & Xie, L. M. (2012). Experimental investigation on temperature of drilling cuttings to predict rock burst. *Chinese Journal of Geotechnical Engineering*, 12, 2822–2832.
- Qiu, L., Song, D., He, X. Q., Wang, E., Li, Z. H. L., Yin, S., et al. (2020). Multifractal of electromagnetic waveform and spectrum about coal rock samples subjected to uniaxial compression. *Fractals*, 28, 2050061.
- Shen, W., Dou, L. Z., He, H., & Zhu, G. A. (2017). Rock burst assessment in multi-seam mining: a case study. *Arabian Journal of Geosciences*, 10, 196.

- Song, D., Wang, E., Li, Z., Qiu, L., & Xu, Z. (2017). EMR: An effective method for monitoring and warning of rock burst hazard. *Geomechanics and Engineering*, *12*, 53–69.
- Song, D., Wang, E., He, X., Jia, H., Qiu, L., Chen, P., & Wang, S. (2018). Use of electromagnetic radiation from fractures for mining-induced stress field assessment. *Journal of Geophysics and Engineering*, *15*, 1093–1103.
- Tang, J. X., Kang, Q. R., & Yang, G. Z. (2010). Application of improved FHAP in mining-disturbed slope stability evaluation. *Disaster Advances*, *3*, 424–427.
- Wang, E. Y., He, X. Q., Dou, L. M., Zhou, S. N., Nie, B. S., & Liu, Z. T. (2005). Electromagnetic radiation characteristics of coal and rocks during excavation in coal mine and their application. *Chinese Journal of Geophysics*, *48*, 216–221.
- Wang, C. (2011). *Research of rock burst risk comprehensive evaluation method based on unascertained measurement model and application*. Dissertation, China University of Mining and Technology.
- Wang, P., Jiang, L. S., Zheng, P. Q., Qin, G. P., & Zhang, C. (2019). Inducing mode analysis of rock burst in fault-affected zone with a hard-thick stratum occurrence. *Environmental Earth Sciences*, *78*, 467.
- Xie, H., Chen, Z., & Wang, J. (1999). Three-dimensional numerical analysis of deformation and failure during top coal caving. *International Journal of Rock Mechanics and Mining Sciences*, *36*, 651–658.
- Zhou, F., Xia, T., Wang, X., Zhang, Y., Sun, Y., & Liu, J. (2016). Recent developments in coal mine methane extraction and utilization in China: a review. *Journal of Natural Gas Science and Engineering*, *31*, 437–458.
- Zhang, Q., Wang, E., Feng, X., Niu, Y., Ali, M., Lin, S., & Wang, H. (2020). Rockburst risk analysis during high-hard roof breaking in deep mines. *Natural Resources Research*, *29*, 4085–4101.